Quaternary Geochronology 33 (2016) 24–34

Contents lists available at ScienceDirect

Quaternary Geochronology

journal homepage: www.elsevier.com/locate/quageo

Research paper

An approach for optimizing *in situ* cosmogenic ^{10}Be sample preparation

Lee B. Corbett [a, *], Paul R. Bierman [a], Dylan H. Rood [b, c]

[a] Department of Geology and Rubenstein School of the Environment and Natural Resources, University of Vermont, Burlington, VT, 05405, USA
[b] Department of Earth Science and Engineering, Imperial College London, South Kensington Campus, London, SW7 2AZ, UK
[c] Center for Accelerator Mass Spectrometry, Lawrence Livermore National Laboratory, Livermore, CA, 94550, USA

ARTICLE INFO

Article history:
Received 12 January 2016
Received in revised form
2 February 2016
Accepted 5 February 2016
Available online 8 February 2016

Keywords:
Geomorphology
Earth surface process
Geochronology
Cosmogenic nuclides
Sample preparation

ABSTRACT

Optimizing sample preparation for the isotopic measurement of ^{10}Be extracted from quartz mineral separates has a direct positive effect on the accuracy and precision of isotopic analysis. Here, we demonstrate the value of tracing Be throughout the extraction process (both after dissolution and after processing), producing pure Be (by optimizing ion exchange chromatography methods and quantifying quartz mineral separate and final Be fraction purity), and minimizing backgrounds (through reducing both laboratory process blanks and ^{10}B isobaric interference). These optimization strategies increase the amount of ^{10}Be available for analysis during accelerator mass spectrometry (AMS), while simultaneously decreasing interference and contamination, and ensuring that sample performance matches standard performance during analysis. After optimization of our laboratory's extraction methodology, $^{9}Be^{3+}$ ion beam currents measured during AMS analysis, a metric for sample purity and Be yield through the extraction process, matched the $^{9}Be^{3+}$ beam currents of AMS standards analyzed at the same time considering nearly 800 samples. Optimization of laboratory procedures leads to purer samples that perform better, more consistently, and more similarly to standards during AMS analysis, allowing for improved precision and accuracy of measurements used for dating and quantification of Earth surface processes.

1. Introduction

Measurement of *in situ* produced cosmogenic ^{10}Be in geologic samples provides insight about a wide variety of geologic processes (Bierman and Nichols, 2004; Gosse and Phillips, 2001; Granger et al., 2013; Nishiizumi et al., 1993; von Blanckenburg and Willenbring, 2014). For example, quantifying ^{10}Be concentrations in moraine boulders (Heyman et al., 2011; Phillips et al., 1990) or previously-glaciated bedrock surfaces (Bierman et al., 1999) provides information about past glacial behavior, thus yielding valuable paleoclimatic insight (Balco, 2011; Fabel and Harbor, 1999). Cosmogenic ^{10}Be is useful for measuring displacement rates on fault systems by dating offset landforms (Bierman et al., 1995; Brown et al., 1998; Matmon et al., 2005; Rood et al., 2010). It can also be employed to study landscape erosion rates, both on outcrop scales (Nishiizumi et al., 1991, 1986) and basin scales (Bierman and Steig, 1996; Brown et al., 1995; Granger et al., 1996; von Blanckenburg, 2005), thereby providing insight about Earth's changing surface (Portenga and Bierman, 2011).

Cosmogenic ^{10}Be forms *in situ* when high-energy cosmic rays bombard rock in the upper-most few meters of Earth's surface (Lal, 1988). In the mineral quartz, ^{10}Be is produced primarily by spallation of oxygen at low rates, on the order of ~4 atoms g^{-1} quartz yr^{-1} at sea level and high latitude (Balco et al., 2008; Borchers et al., 2016). Production of ^{10}Be in rock and soil is primarily dependent on latitude and elevation, and effectively ceases if the sample surface is buried to a depth of more than a few meters (for example, by glacial ice, sediment, or soil). ^{10}Be has a half-life of ~1.4 million years (Chmeleff et al., 2010; Korschinek et al., 2010; Nishiizumi et al., 2007). Therefore, while concentrations of ^{10}Be initially increase in exposed rock over time, they eventually level off as production, erosion, and decay reach steady state.

Preparing and analyzing a sample for ^{10}Be measurement requires numerous steps. After a sample is collected, the mineral quartz is isolated from the other mineral phases through a series of physical and chemical processes (Kohl and Nishiizumi, 1992). The quartz is then dissolved in the presence of a ^{9}Be carrier solution, and Be is chemically isolated. To measure ^{10}Be, atoms of this rare

* Corresponding author.
E-mail address: Ashley.Corbett@uvm.edu (L.B. Corbett).

http://dx.doi.org/10.1016/j.quageo.2016.02.001
1871-1014/

isotope are counted in relation to the ion current of stable ^{9}Be via accelerator mass spectrometry, or AMS (Muzikar et al., 2003; Tuniz et al., 1998). Because isotopic fractionation can occur in the AMS, primary standards such as the KNSTD dilution series (Nishiizumi et al., 2007) are analyzed in association with samples. A correction factor for the measured versus the assumed ^{10}Be/^{9}Be ratio of primary standards is determined, then applied to normalize ratio measurements for samples analyzed at the same time.

The accuracy of sample measurement is controlled in part by the overall closeness of match between standards and samples. Developing a correction factor from standard ^{10}Be/^{9}Be ratios and using it to normalize sample ^{10}Be/^{9}Be ratios relies upon the assumption that standards and samples behave similarly during measurement. Important characteristics may include matrix effects (e.g. accessory elements that could interfere with measurement; Hunt et al. (2008), Merchel et al. (2008)), cathode geometry (e.g. depth to the sputtering surface and shape of the surface; Hunt et al. (2007), Rood et al. (2013), Shanks and Freeman (2015)), total mass, and performance during measurement (the ion source yield, or "beam current", which we measure as the $^{9}Be^{3+}$ current but which can alternatively be measured as the $^{9}Be^{16}O^{-}$ current). The similarity of beam currents between standards and samples across multiple measurement cycles is particularly important (Rood et al., 2014). Additionally, contamination of a sample with the isobar ^{10}B, above the ability of the detector to reject such interference, inhibits reliable detection of ^{10}Be and has the potential to degrade accuracy (Merchel et al., 2012).

The precision of low ^{10}Be/^{9}Be samples is primarily controlled by Poisson counting statistics, with greater numbers of ^{10}Be counts yielding more precise analyses. The total number of attainable counts is a product of the ^{10}Be concentration of the material being analyzed, the total mass of the sample, and the AMS total system efficiency (including ionization, transmission, transport, and detection efficiencies), all of which dictate the number of ^{10}Be counts that can be obtained before the sample material is ablated away during sputtering (Rood et al., 2013, 2010). For higher ^{10}Be/^{9}Be samples, precision is primarily controlled by the reproducibility (i.e., scatter) of ratio measurements, which is often poorer than that predicted by counting statistics alone (Rood et al., 2013). For these higher ^{10}Be/^{9}Be samples that are limited by reproducibility rather than counting statistics, closeness of match to standards can dictate precision in addition to accuracy (Rood et al., 2014). Background levels of ^{10}Be introduced during sample processing also control the precision of measured isotopic ratios, with relatively higher process blanks increasing the uncertainty of sample ^{10}Be/^{9}Be ratios especially in samples with little ^{10}Be, because background uncertainties are typically added in quadrature.

There are several reasons why it is advantageous to optimize the preparation of samples for ^{10}Be isotopic analysis. Ensuring that sample performance matches standard performance during AMS analysis likely increases the accuracy of sample measurements, a prerequisite for accurate determination of dates and rates across a variety of applications. Increasing the precision of analyses enhances not only the interpretations that can be made from dates and rates, but also enables approaches involving multiple isotopic systems such as burial dating (Granger and Muzikar, 2001) and isochron burial dating (Balco and Rovey, 2008), and allows for improved calibration of cosmogenic nuclide production rates (Balco et al., 2009; Borchers et al., 2016; Briner et al., 2012; Putnam et al., 2010). Very low concentration samples, such as those from young exposures (Licciardi et al., 2009), rapidly eroding landscapes (Portenga et al., 2015), or long-buried sediments (Erlanger et al., 2012; Gibbon et al., 2014), require low detection limits to be measurable above background levels. High $^{9}Be^{3+}$ beam currents reduce the counting times required to achieve desired precisions, thereby speeding AMS throughput and better utilizing the limited beam time available for analysis.

This paper discusses optimization of the Be extraction procedure (Fig. 1) used at the University of Vermont, with the aim of increasing data accuracy and precision as well as the efficiency of sample preparation and AMS analysis. Our goal is to produce pure samples of Be that match the performance of standards, with particular focus on obtaining high Be yield, consistent $^{9}Be^{3+}$ beam currents, low and consistent ^{10}Be/^{9}Be background levels, and minimal isobaric interference. The optimization strategies discussed here are generalizable to other laboratories as well as to other AMS facilities.

2. Brief history of ^{10}Be extraction and measurement

Over time, different methods have been used to measure terrestrial cosmogenic ^{10}Be. Initially, abundances of cosmogenic ^{10}Be were quantified by radioactive decay counting after Be was isolated from silicate minerals by dissolution in acid (Fairhall, 1960). However, only samples with the highest ^{10}Be concentrations, for example those exposed at high elevations for long durations, could be measured. Later, it became possible to measure ^{10}Be/^{9}Be ratios via AMS (Lanford et al., 1980; Raisbeck et al., 1978; Southon et al., 1983; Thomas et al., 1981; Turekian et al., 1979), including on lower-energy AMS systems (Raisbeck et al., 1987). Be yields from chemical preparation were typically high (85–90%), but samples frequently retained impurities, especially Al (Lanford et al., 1980). At that time, precisions were generally 5–10%, and detection was limited to ^{10}Be/^{9}Be ratios greater than ~10^{-13} (Southon et al., 1983).

Although measurements of ^{10}Be became more common into the 1980's, average AMS beam currents remained relatively low (Klein and Middleton, 1984). By 1990, the quality of AMS measurements of ^{10}Be increased, and precisions of several percent were attainable (Suter, 1990). At around the same time, *in situ* ^{10}Be became a more widely used dating technique as AMS analysis improved and after it was confirmed that meteoric ^{10}Be produced in the atmosphere and adhered to the surface of grains could be removed from the grain coatings of a sample with repeated acid etches (Brown et al., 1991; Kohl and Nishiizumi, 1992; Nishiizumi et al., 1991, 1986, 1989). Adding column chromatography to the extraction protocol ensured that Be could be cleanly separated from other elements (Ditchburn and Whitehead, 1994; Tera et al., 1986).

Recent methodological advances have further increased the quality of AMS ^{10}Be measurements by improving beam currents. BeO had traditionally been mixed with Ag before being packing into cathodes for AMS analysis; however, using Nb instead of Ag increased $^{9}Be^{3+}$ beam currents (Hunt et al., 2006; Merchel et al., 2008). It is uncertain whether impurities in the final Be fraction decrease AMS $^{9}Be^{3+}$ beam currents beyond dilution effects. Merchel et al. (2008) suggested that additions of Ti did not directly decrease $^{9}Be^{3+}$ beam currents, although the resulting dilution of Be did. However, Hunt et al. (2008) found that Al and Ti both depressed $^{9}Be^{3+}$ beam currents beyond the effects of dilution (although Ca, Fe, Mg, and Mn did not).

Detection limits have also improved over the past several decades. The discovery that commercial aluminum often contains non-negligible amounts of ^{10}Be occasioned the use of stainless steel and copper cathodes for sample analysis (Middleton et al., 1994), lowering backgrounds. Although commercially-available ^{9}Be carrier is commonly used, its ^{10}Be/^{9}Be ratio is ~10^{-14}, which hinders the analysis of low-level samples. In contrast, ^{9}Be carriers made from deeply-mined phenakite (Be_2SiO_4) and beryl ($Be_3Al_2Si_6O_{18}$) often yield ^{10}Be/^{9}Be ratios two orders of magnitude lower (Merchel et al., 2008), which are better suited for the analysis of low-level

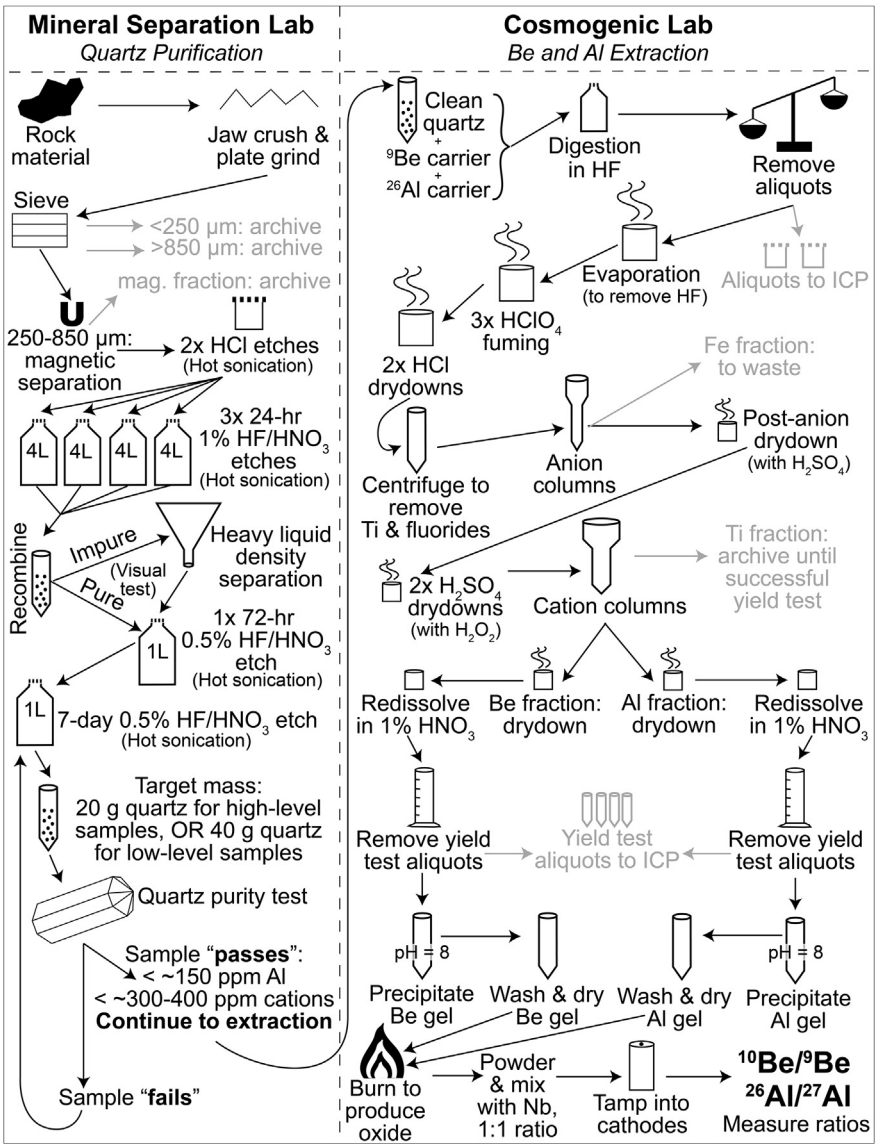

Fig. 1. Flow chart of Be isotopic sample preparation at the University of Vermont. Arrows designate the direction of sample progression through the process, and gray font indicates sample fractions removed from the flow.

samples. Experiments at Lawrence Livermore National Laboratory suggests that the AMS detection limit is now as low as ~1000 total ^{10}Be atoms in a sample (or ~10 ^{10}Be counts, assuming a 1% total AMS efficiency) as long as backgrounds are low, making it possible to obtain high-precision measurements on small samples or samples with little ^{10}Be (Rood et al., 2010). Samples with as few as several hundred ^{10}Be atoms g^{-1} quartz, the equivalent of less than 100 years of surface exposure at sea level and high latitude, can now be measured above background (Corbett et al., 2015).

3. Background and study design

In 2008, a new cosmogenic extraction laboratory was built at the University of Vermont. The laboratory was designed to maximize sample throughput, minimize isobaric boron (^{10}B) interference, and provide a clean workspace so as to lower ^{10}Be/^{9}Be backgrounds. While developing the new laboratory space, we refined the sample preparation methodology that the laboratory had used for more than a decade (Hunt et al., 2008). The goal was to produce pure, high-yield samples of BeO that consistently performed similarly to standards during AMS analysis in order to maximize both accuracy and precision.

During the first half of 2009, we tested and refined sample processing procedures (Fig. 1). We focused on three parts of the procedure: tracing beryllium through the extraction process to maximize yield, improving ion exchange chromatography column performance to generate high-purity Be, and reducing backgrounds to improve detection limits. From 2009 to 2012, five University of Vermont graduate students, three laboratory visitors, and a faculty member processed ~800 *in situ* ^{10}Be samples in the new laboratory using these modified procedures and then measured the samples by AMS at Lawrence Livermore National Laboratory. Here, we use data from these ~800 samples to make inferences about the effectiveness of methodological optimization following the guidance provided by Hunt et al. (2008).

We use ^{9}Be^{3+} beam currents of samples as our primary, first-order metric for quantifying sample performance during AMS analysis. For the sake of consistency between samples, which were counted between two and four separate times depending on the ^{10}Be/^{9}Be ratio and desired precision, we report the average ^{9}Be^{3+}

beam current of the first two 300-s counting cycles of each sample. We present both measured beam currents (μA) as well as normalized beam currents in order to remove run-to-run variability in AMS tuning and source performance. We normalized sample beam currents to the average beam current from the first run of all (both primary and secondary) standards on the same wheel. A normalized current of 1.0 indicates that the sample performed as well as the standards, a normalized current of less than 1.0 indicates that the sample did not perform as well as the standards, and a normalized current of greater than 1.0 indicates that the sample outperformed the standards.

Much of our analysis and discussion focuses on cation exchange column chromatography, which removes B and Ti and separates Be from Al (Clifford, 1999; Ochs and Ivy-Ochs, 1997). The rate at which Ti, Be, and Al elute through cation exchange columns depends on multiple factors including column geometry, resin type, resin mesh size, resin bed volume, and acid strength (Clifford, 1999). In our discussion of sample purity and column chromatography, we report both the total mass of the ions of interest (in μg) as well as their charge equivalents (in milli-equivalents, or meq, where one meq is equal to one millimole of charge). For example, for Al, which forms a +3 cation and has a molar mass of ~27 g mol^{-1}, 1000 μg Al is equivalent to 0.11 meq; for Ti, which forms a +4 cation but has a greater molar mass (~48 g mol^{-1}), 1000 μg Ti is equivalent to 0.08 meq.

4. Methods

4.1. Laboratory design and method development

We optimized laboratory design to minimize background levels of ^{10}Be and isobaric ^{10}B. Air is supplied to the laboratory by a dedicated air handler with three filtration stages (35% and 90% boron-free polypropylene filter media, followed by diffuser-mounted Ultra Low Particle (ULPA) filters made of synthetic material). Each fully exhausting laminar flow fume hoods draws ambient air from the laboratory; this air is again 35% and ULPA filtered before entering the hoods and all lab air is exhausted rather than recirculated. Although the laboratory was not built to a specific cleanroom standard, particle tests run during operation indicate that laboratory air contains about 0.2 particles per cubic centimeter, consistent with a class 100 to class 1000 cleanroom. Only deionized water (17.3–17.7 Mohm) is supplied to the laboratory; before the water is used for dilution or washing, it is polished using Milli-Q deionization units equipped with boron-specific, Q-gard cartridges. We use two fully separate processing streams with dedicated labware and hood space to separate high-level samples ($^{10}Be/^{9}Be > 10^{-13}$) from low-level samples ($^{10}Be/^{9}Be < 10^{-13}$).

We also optimized laboratory design to minimize ambient boron levels. Fiberglass insulation was replaced by foam and rock wool, and prefabricated aluminum wall panels were used in place of sheetrock. We used water leaching to test all laboratory materials and, finding detectable boron in most paper and cardboard products, have minimized their use in the lab and in air filtration materials.

We designed the laboratory to have perchloric-acid compatible fume hoods with a washdown system. Post-dissolution high-temperature sample fuming with perchloric acid breaks down insoluble fluoride compounds and evaporates residual fluorides (Ochs and Ivy-Ochs, 1997), which can negatively impact the cation column elution curve if they persist in samples.

To minimize acid consumption and to speed throughput, we use 3 mL anion columns (Dowex 1X8 200–400 mesh resin, 1.2 meq mL^{-1}, total capacity = 3.6 meq) and 5 mL cation columns (Dowex 50WX8 200–400 mesh resin, 1.7 meq mL^{-1}, total capacity = 8.5 meq). We use double-fritted columns for both (Fig. 2); the second frit sits 1–2 mm above the resin bed and maintains a thin layer of solution between the top of the resin bed and the bottom of the second frit.

We repeatedly tested column performance before processing samples using quartz digests spiked with differing concentrations of additional Al and Ti. During the earlier tests, the goal was to determine the most effective way to separate the three primary elution peaks (Ti, Be, and Al) by experimenting with acid strength and elution volume, and collecting all of the eluted solution for Inductively-Coupled Plasma Optical Emission Spectrometry (ICP-OES) analysis (Fig. 3). To ensure that samples are Ti-free, we continue Ti elution until all Ti is removed, even if small amounts of Be (several percent of the total load) may be lost. We add hydrogen peroxide to the sample before column chromatography which stains the Ti red, providing a visual confirmation that it has been completely removed before Be elution begins (Clifford, 1999).

After optimizing the column elution procedure, later tests were targeted at determining the total cation load (charge equivalent) that the columns could handle by spiking quartz to various impurity levels and determining the threshold of column failure. Column failure occurred when elements eluted prematurely, contaminating the Be fraction with both Ti and Al (Fig. 3). In our experiments, failure occurred at ~10% capacity, or ~0.85 meq for the cation columns. For Al (+3 charge, ~27 g mol^{-1} molar mass), this equates to 7650 μg; for Ti (+4 charge, ~48 g mol^{-1} molar mass), this equates to 10,200 μg (however, actual quartz contains many different cations).

4.2. Quartz purity and sample massing

Rock samples are crushed, ground, and sieved, while sediment samples are just sieved. To isolate quartz from other mineral phases, we use magnetic separation, repeated acid etches, and density separation if necessary (Kohl and Nishiizumi, 1992). After etching,

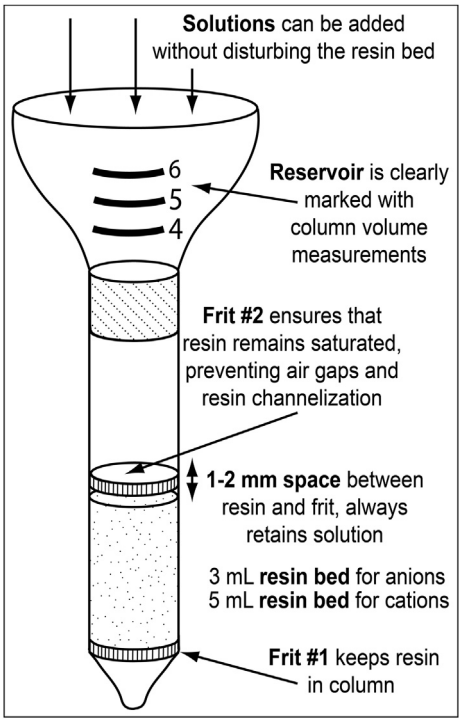

Fig. 2. Diagram of a double-fritted column implemented for both anion and cation chromatography methods.

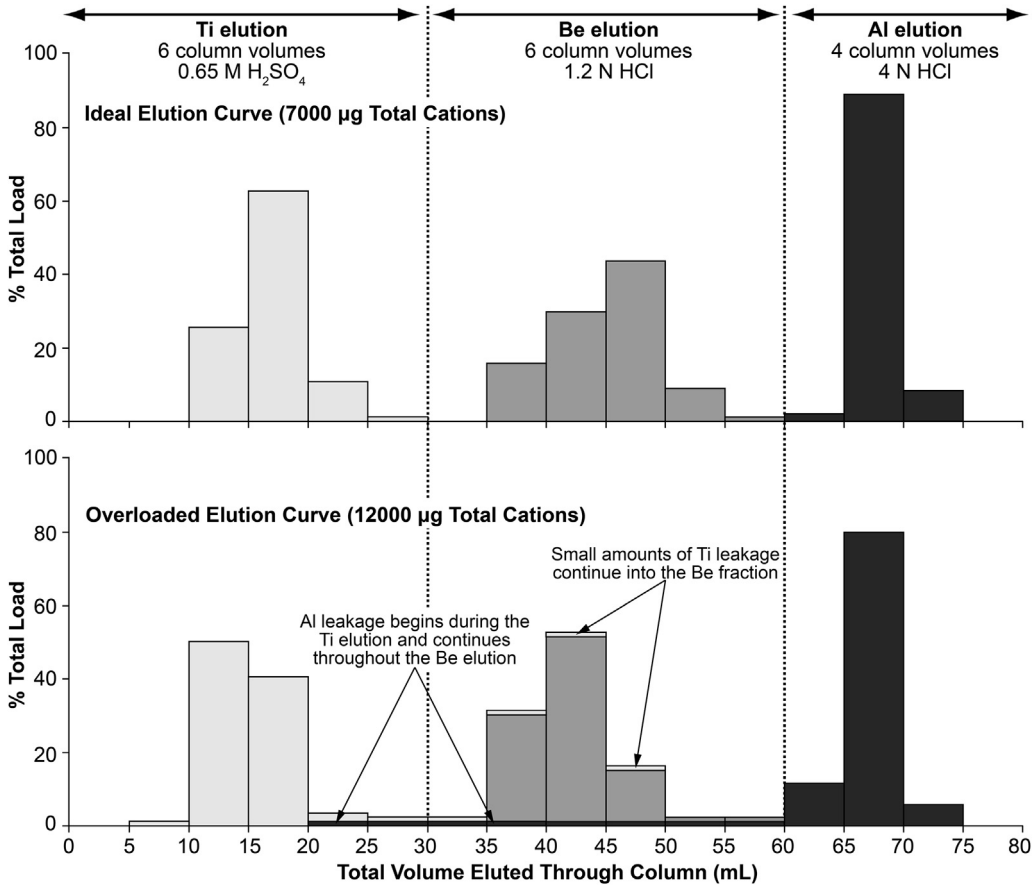

Fig. 3. Cation chromatograms from tests performed during method development. Ti, Be, and Al are shown in light gray, medium gray, and dark gray, respectively. Top pannel shows an optimized elution curve that cleanly separates the three fractions (total cation load of 7000 µg). Bottom pannel shows an overloaded elution curve (total cation load of 12,000 µg).

0.25 g aliquots of purified quartz are dissolved in concentrated HF and tested for purity with regard to major elements (Al, Ca, Fe, K, Mg, Na, and Ti) using a rapid ICP-OES method. Quartz with high impurity levels is re-etched for an additional week, then tested again.

We use quartz cation concentrations to decide how much sample can be dissolved without overloading the ion exchange columns. Because our experimentation has shown that cation column failure occurs at ~10% of the total resin capacity, we limit the amount of quartz we dissolve based on its purity such that we load only ~0.85 meq to our 5 mL cation columns. This is a conservative approach because perchloric acid treatments oxidize much of the Ti (Hunt et al., 2008), which is later removed by centrifugation. We use up to ~20 g of quartz for high-level samples ($^{10}Be/^{9}Be > 10^{-13}$) and up to ~40 g of quartz for low-level samples ($^{10}Be/^{9}Be < 10^{-13}$); these upper limits for quartz mass were chosen based on the capacity of the Teflon labware we use for dissolution and extraction.

To the quartz, we add 250 µg ^{9}Be via in-house made beryl-derived carrier solution. Additions of ^{27}Al (via SPEX Al standard) are determined based on the quantified native Al in the quartz, with the aim of having ~2000 µg Al in each sample. We digest samples in HF (~5 g HF per g quartz) over several days, increasing the digest temperature incrementally up to 135 °C.

4.3. Blanks

Each batch of ten samples includes one blank and one CRONUS standard for high-level samples ($^{10}Be/^{9}Be > 10^{-13}$) and two blanks for low-level samples ($^{10}Be/^{9}Be < 10^{-13}$). We currently use ^{9}Be carrier made in-house by the flux fusion of beryl (Stone, 1998) for all samples; however, the earliest high-level samples had blanks of SPEX brand 1000 ppm ICP elemental standard. All of these process blanks as well as samples contain ~250 µg ^{9}Be.

4.4. Post-dissolution aliquots

Immediately following dissolution, we remove replicate aliquots directly from the HF digestion solution, quantifying the percentage of solution removed by mass. These aliquots represent ~2% and 4% of the total sample mass, respectively. To each aliquot we add a small amount of H_2SO_4 to ensure the aliquot does not reach dryness, evaporate the HF, and then add (by mass) a 1% H_2SO_4 solution spiked with Ga and Y to act as internal standards and correct for instrument drift. We use these aliquots to quantify Be and Al at high precision (percent level) with ICP-OES, using multiple measurement lines for each element (Be, 234.861 and 249.473 nm; and Al, 308.215 and 309.271 nm).

4.5. Be isolation and post-processing aliquots

Following removal of post-dissolution aliquots, we evaporate the remaining HF and fume the samples three separate times with perchloric acid at 230 °C to break up and drive off fluoride compounds (Ochs and Ivy-Ochs, 1997). We then centrifuge samples to remove Ti and insoluble fluorides, convert samples to chloride form by fuming with and dissolving in HCl, and perform anion column chromatography to remove Fe. After anion column chromatography, we evaporate the HCl, convert samples to sulfate form, and

perform cation column chromatography to remove B and Ti and separate Be from Al (Clifford, 1999; Ochs and Ivy-Ochs, 1997).

At the end of the extraction process and before hydroxide precipitation, we test the Be fraction for yield and purity by extracting small aliquots. Because we employ a volumetric dilution and a rapid ICP-OES method to speed the process, the precision of these data is less than that of the post-dissolution aliquots. Samples are then precipitated as Be hydroxide at pH ~8 (using methyl red, a liquid pH indicator), dried, converted to BeO using an air/wall gas flame, mixed with Nb at a 1:1 M ratio (Hunt et al., 2006), and packed into stainless steel cathodes for AMS analysis.

5. Results

5.1. Quartz purity

Quartz purity varies appreciably between study sites. Of the 797 quartz samples tested during 2009–2012, the average total cation concentration was 333 ± 359 μg g^{-1} (1SD) in terms of mass, or 0.024 ± 0.038 meq g^{-1} (1SD) in terms of charge (Fig. 4). On average, almost half of this concentration is comprised of Al (119 ± 117 μg g^{-1}, or 0.013 ± 0.013 meq g^{-1}, 1SD, Fig. 4). However, since Fe is removed during anion column chromatography, the effective total load during cation chromatography excludes Fe and averages 272 μg g^{-1} (0.021 meq g^{-1}).

5.2. Post-dissolution aliquots

Because samples have only been dissolved at the point we remove these aliquots and there is no mechanism for Be loss, post-dissolution aliquots should return 100% of the Be that was added to the sample through ^{9}Be carrier (plus any native ^{9}Be contained within the quartz).

Aliquot measurements of blanks yielded 100.7 ± 2.1% (mean, n = 114, 1SD) of the expected Be based on the mass and concentration of ^{9}Be carrier added (Fig. 5a). This value suggests that our ICP-OES precision for Be measurements in this context is ~2% (1SD), which is greater than the uncertainty of individual ICP replicates (usually ≤ 1%) but similar to nominal precision of many AMS ^{10}Be analyses at present (Rood et al., 2013). Aliquot measurements of blanks are normally-distributed.

Aliquot measurements of samples are more variable than those of the blanks and have a long-tailed distribution skewed toward higher values. Quantification of Be in samples yielded an average of 100.8 ± 22.4% (mean, n = 797, 1SD) of the expected Be based on the mass and concentration of ^{9}Be carrier added (Fig. 5b).

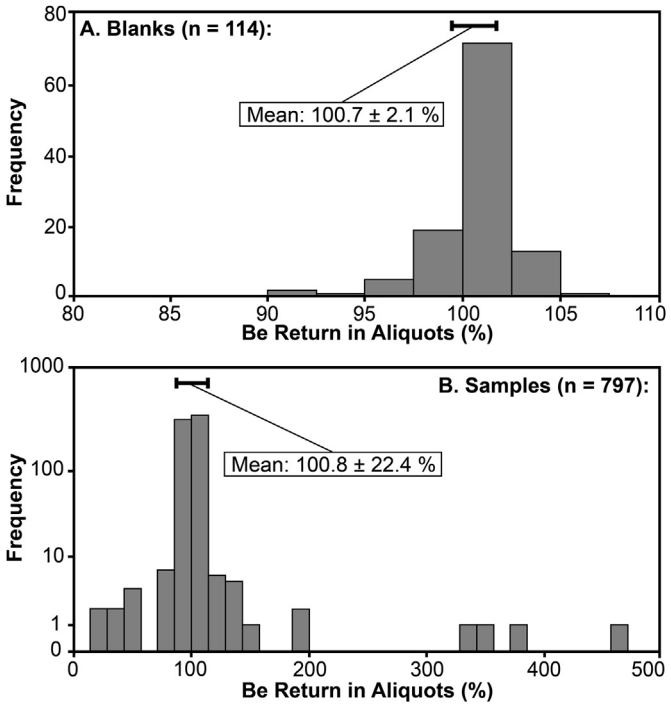

Fig. 5. Histograms of Be measurements from ICP-OES aliquots taken from samples directly following dissolution. Top panel shows data for blanks (n = 114) and bottom panel shows data for samples (n = 797; note log scale on y-axis). Since no processing (except dissolution) has occurred at this point in the process, samples should return 100% of the expected Be. Samples containing more than 100% of the expected Be likely contain native ^{9}Be. Thick bar shows average ± 1SD.

5.3. Post-processing aliquots

For the post-processing aliquots, Be yield should be 94% because 6% of the total sample is removed for the post-dissolution aliquots. For the process blanks, the measured Be yield is 94.0 ± 3.6% (mean, n = 114, 1SD, Fig. 6a) of the total Be based on the mass and

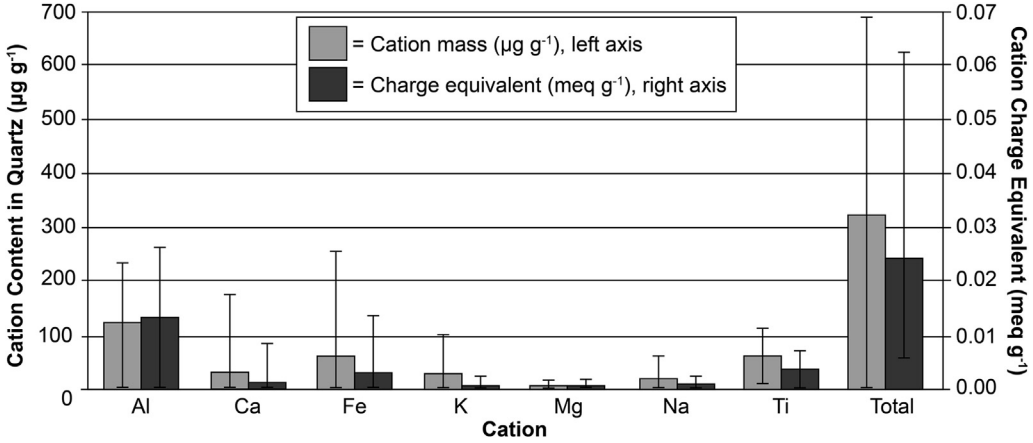

Fig. 4. Average cation concentrations in quartz analyzed during 2009–2012 (n = 797), expressed both in terms of mass (μg g^{-1}, light gray bars, left axis) and charge equivalent (meq g^{-1}, dark gray bars, right axis). Error bars show ± one standard deviation. The total capacity of our 5 mL cation columns is 8.5 meq, and we determined that column failure occurred at ~10% capacity (0.85 meq). Assuming we use 20 g of average quartz shown here (0.021 meq g^{-1} excluding Fe, which is removed during anion column chromatography), then our columns are on average operating half-way (0.42 meq) to their failure capacity.

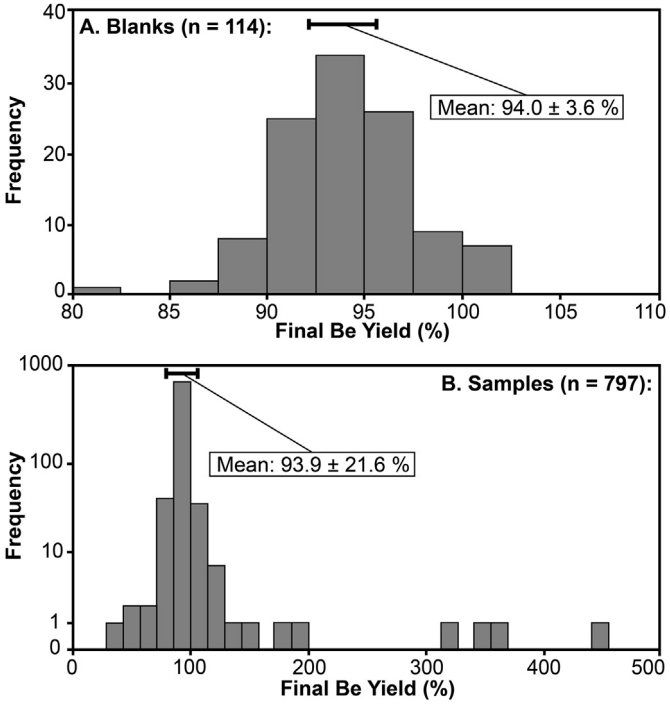

Fig. 6. Histograms of Be measurements from ICP-OES aliquots taken from samples just before final precipitation. Top panel shows data for blanks (n = 114) and bottom panel shows data for samples (n = 797; note log scale on y-axis). Since 6% of the sample was removed in the first set of aliquots, final yields should be 94%. Samples containing more than 94% of the expected Be likely contain native ^{9}Be. Thick bar shows average ± 1SD.

concentration of ^{9}Be carrier added. For samples, the measured Be yield is 93.9 ± 21.6% (mean, n = 797, 1SD, Fig. 6b) of the total. When considered in reference to the quartz that was dissolved, laboratory treatment of Be fractions decreased average total sample Al contents by 99.1%, Fe contents by 99.5%, and Ti contents by 99.9% (n = 797, Fig. 7).

5.4. Background ^{10}Be/^{9}Be ratios

Measured isotopic ratios of process blanks reflect the type of carrier used in their preparation and the average ^{10}Be concentration of samples processed in the batches accompanying the blanks. Beryl blanks are lower ($5.6 \pm 3.2 \times 10^{-16}$, 1SD, n = 59) in the hood used to process low-level samples and higher ($9.0 \pm 8.9 \times 10^{-16}$, 1SD, n = 29) in the hood used to process high-level samples (Fig. 8). When assessed in an unequal variance Student's T-Test, beryl blank ratios between the two hoods are statistically separable (p = 0.004). SPEX carrier blanks in the high-level hood have an average ratio more than an order of magnitude higher than beryl blanks in the same hood ($1.2 \pm 0.1 \times 10^{-14}$, 1SD, n = 19, Fig. 8). When assessed in an unequal variance Student's T-Test, the ratios of the SPEX blanks and the beryl blanks processed in the same hood are statistically separable (p < 0.001).

For beryl blanks processed in the low-level hood, the standard deviation of the 59 different measurements (57%) is larger than the average measurement uncertainty (36%). For beryl blanks processed in the high-level hood, the discrepancy between the standard deviation of the 29 measurements (82%) and the average measurement uncertainty (29%) is greater. For SPEX blanks processed in the high-level hood, the standard deviation of the 19 measurements (4%) is less than the average measurement uncertainty (7%), although both values are appreciably smaller than for beryl blanks because there are more ^{10}Be counts resulting in more precise data. Over time (2009–2012), there appears to be no trend in process blank ^{10}Be/^{9}Be ratios (Fig. 9).

5.5. Sample beam currents

The AMS $^{9}Be^{3+}$ beam currents of samples were consistent for samples processed during 2009–2012 (Fig. 10). The average beam current for samples was 21.4 ± 3.8 μA (1 SD, n = 797). The beam current normalized to standards run with these samples averaged 1.0 ± 0.2 (1 SD, n = 797). Quartz purity (expressed as total cation

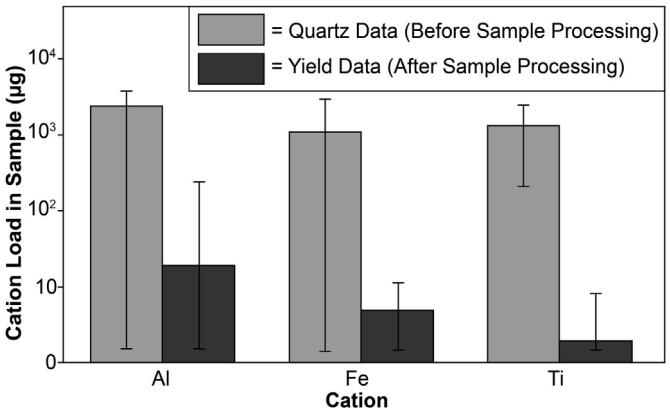

Fig. 7. Final cation contents in Be fractions (from post-processing aliquots; black bars) compared to initial total cation contents in quartz (from quartz test data; gray bars; obtained by multiplying the concentration of cations in quartz by the mass of quartz used for each sample). Y-axis is in logarithmic scale.

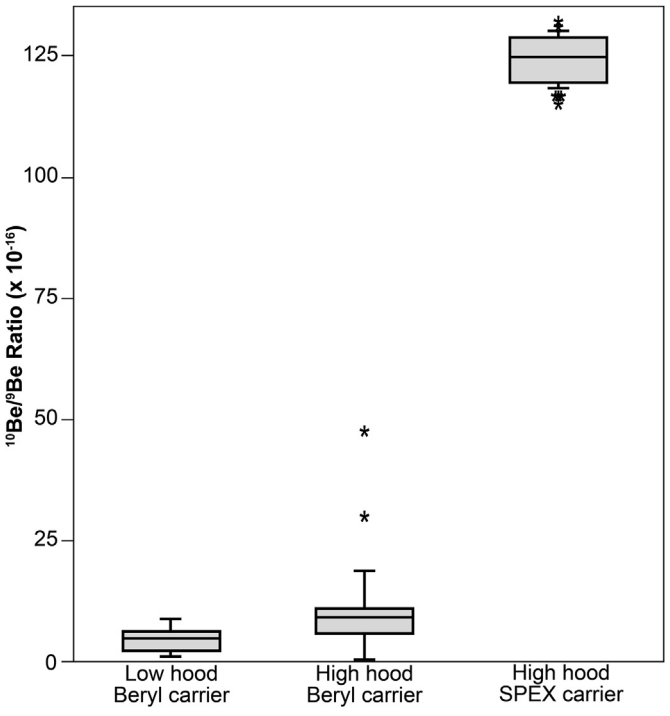

Fig. 8. Box and whisker plots of process blanks from three different scenarios: beryl carrier in the low-level hood (n = 59), beryl carrier in the high-level hood (n = 29), and SPEX carrier in the high-level hood (n = 22). The box encloses the area between the first and third quartiles and the horizontal line represents the median. Whiskers show one standard deviation. Samples that lie outside one standard deviation from the mean are shown with an asterisk.

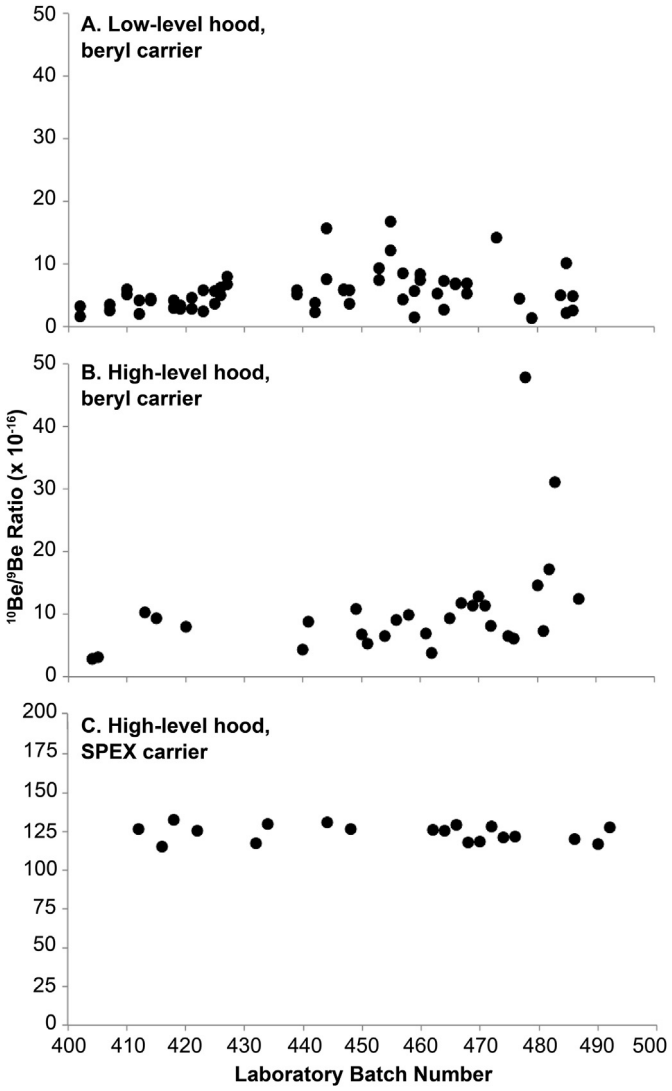

Fig. 9. Blank ^{10}Be/^{9}Be ratios from 2009 to 2012 from three different scenarios: beryl carrier in the low-level hood (A; n = 59), beryl carrier in the high-level hood (B; n = 29), and SPEX carrier in the high-level hood (C; n = 22).

load) is not significantly related to normalized sample $^{9}Be^{3+}$ beam current ($R^2 = 0.004$, $p = 0.066$) indicating that our optimized laboratory methods are able to compensate for a wide range of initial quartz impurity concentrations.

Analysis of $^{9}Be^{3+}$ beam currents also indicates that the methods we describe here yield more predictable sample performance than those used previously in the University of Vermont cosmogenic nuclide laboratory. A previous assessment of data quality by Hunt et al. (2008) showed a greater range of beam currents, yielding a relative standard deviation of ~40% (n = 63). The beam current data we show here have a relative standard deviation of 18% (n = 797).

6. Discussion

6.1. Tracing beryllium through the extraction process

Tracing Be throughout the extraction process provides insight about the samples at two steps. Analysis of post-dissolution aliquots (Fig. 5) quantifies if any native ^{9}Be is present in the quartz (Portenga et al., 2015), while analysis of post-processing aliquots

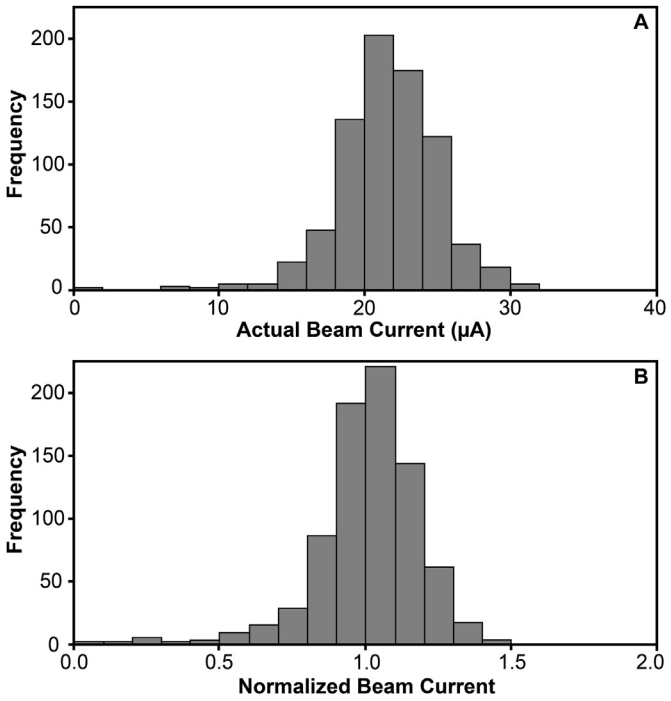

Fig. 10. AMS $^{9}Be^{3+}$ beam currents (n = 797). Top pannel shows beam currents (μA) measured on the Lawrence Livermore National Laboratory AMS. Bottom pannel shows sample beam currents normalized to standard beam currents.

(Fig. 6) serves as a quality control metric to assess final Be yield and ensure that all samples have consistent Be mass (Hunt et al., 2008). Rare departures from the expected values for these two parameters may indicate the need for corrections, either accounting for native ^{9}Be in the data reduction or identifying and remediating sources of Be loss.

For the post-dissolution aliquots (Fig. 5), which should return 100% of the expected Be based on carrier addition, the few samples more than 2% (the 1SD precision of our analyses based on the performance of the blanks) below the central tendency likely reflect massing errors or ICP-OES interferences from rare accessory elements in quartz. Samples more than 2% (1SD, based on analysis of blanks) above the central tendency are those in which the quartz likely contained native ^{9}Be. For the post-processing aliquots (Fig. 6), which should return 94% Be yield, samples considerably below 94% may be a result of laboratory error (for example, spilling a sample) and/or limitations during measurement such as interfering peaks. Samples falling considerably above 94% Be yield likely indicate the presence of ^{9}Be in quartz, which can be verified by cross-checking against the higher-precision post-dissolution aliquot measurements.

Be tracing unambiguously demonstrates the presence of native ^{9}Be in some purified quartz mineral separates (Figs. 5b and 6b) and allows the mass of native ^{9}Be to be incorporated in the calculation of ^{10}Be concentrations derived from the measured ^{10}Be/^{9}Be ratio. Although our ability to detect small amounts (few μg) of native Be is limited by the overall precision of ICP-OES analysis (~2% for the post-dissolution aliquots, as described above), such small additions of native Be are less important as they do not change calculated ^{10}Be concentrations beyond the precision of the AMS measurements. Because the method we use can reliably detect larger amounts (>10 μg) of native Be, an amount which begins to impact the resulting data at the several percent level, we can correct for its presence. Considering the dataset assessed here (Fig. 5b), 56 of the 797 samples (or ~7% of the population) exceed the expected Be

measurement by 2 SD (4%) and 38 of the 797 samples (or ~5% of the population) exceed the expected Be measurement by 3 SD (6%).

Failing to identify and correct for native Be in those samples for which quartz contributes more than a few μg of Be would have caused errors in the calculation of ^{10}Be concentration and thus in the inferred erosion rates, exposure ages, and dual isotope ratios. For example, in a suite of 49 samples from Bhutan prepared at University of Vermont, most samples contained detectable native ^{9}Be (Portenga et al., 2015). Approximately 240 μg of ^{9}Be carrier was added to each of the Bhutan samples as a spike; however, ICP-OES analysis of aliquots demonstrated that samples contained 244–1158 μg total ^{9}Be, indicating native ^{9}Be loads of as much as 900 μg per sample and native ^{9}Be concentrations in quartz as high as 38 μg g^{-1} (see Fig. 3 in Portenga et al. (2015)). These native ^{9}Be concentrations are as much as 4–5 times greater than the amount of ^{9}Be carrier added. The source of this native Be may include beryl crystals, fluid inclusions in quartz grains, and/or structural substitution in quartz grains (Grew, 2002). Failure to detect and correct for this native ^{9}Be would have caused erosion rate overestimates of as much as 400% (Portenga et al., 2015).

Post-processing aliquots (Fig. 6) serve as a quality check at the end of the extraction procedure to verify that samples are ready for AMS analysis and provides quality control in a laboratory where many different people each year are preparing samples. Quantifying the Be yield determines if enough Be is present for a successful AMS measurement. If sufficient Be is not present in the sample, the Ti fraction is analyzed by ICP-OES; in this case (which has happened only once when elution acid was incorrectly mixed), the missing Be eluted through the cation column early and was recovered by reprocessing the Ti fraction.

6.2. Producing pure beryllium

Creation of high-purity Be fractions ensures that samples will perform similarly to the standards during AMS analysis and provides a constant mass of material to load into cathodes. We demonstrate here that Be purity can be maximized by improving and calibrating/verifying column chromatography methods, tailoring the mass of quartz so as not to overload the columns, and verifying purity via quality control post-processing aliquots (Fig. 7). Constant ^{9}Be mass results in a uniform depth to the material surface and a consistent mixing ratio with Nb, which optimizes the ionization yield, the AMS sputtering efficiency, and the measurement reproducibility (Rood et al., 2010, 2013) for sputter sources using front-loaded cathodes.

Optimized column methodology improves data quality and reduces the time needed to make AMS measurements. After cation column chromatography, post-processing aliquots show that Be fractions are consistently free of impurities (Fig. 7), contain virtually all of the original Be (Fig. 6), and that the resulting ^{9}Be^{3+} beam current is not related to the purity of the quartz. Even in small concentrations, Ti is thought to diminish ^{9}Be^{3+} beam currents beyond the dilution effects (Hunt et al., 2008). If Al, Fe, or Ti are present at greater than trace levels (>100 μg for Al, Fe, and Ti) in the post-column Be fraction, which occurs only rarely, the Be fraction can be neutralized, precipitated, re-dissolved, and cycled through anion and/or cation columns a second time to remove remaining impurities. We are unable to definitively address the impact of Ti on ^{9}Be^{3+} beam currents with our dataset since we have successfully removed Ti from the samples described here (Fig. 7) and hence do not have a range of Ti values over which to assess resulting beam currents.

The double-fritted column configuration (Fig. 2) has several benefits. The second frit prevents the column from drying out during the elution process, thereby avoiding channeling which can allow solution to bypass the resin. In addition, the second frit ensures that the resin bed is not disturbed while adding solutions, allowing the column steps to be performed in a more time-efficient and reproducible manner; cation column chromatography on a batch of 12 samples can be performed in 3–4 h. These double-fritted columns have successfully been regenerated and re-used for several years (more than 50 batches of samples) by stripping them with acid, flushing them with water, and storing them fully saturated in water between uses. Over that time, there has been no change in column performance or blank values.

6.3. Reducing backgrounds to improve detection limits

Backgrounds are an important control on the accuracy and precision of ^{10}Be analyses, especially for samples with low ^{10}Be/^{9}Be ratios. Improved AMS techniques now consistently produce machine blanks with ^{10}Be/^{9}Be ratios well below 10^{-15} (Rood et al., 2010), placing greater demands on processing laboratories to both minimize sample cross-talk and lower the amount of the interfering isobar, ^{10}B.

Using beryl carrier and processing low-level samples in a separate fully-exhausting laminar flow hood with dedicated labware resulted in blanks almost two orders of magnitude lower than using commercial carrier (Figs. 8 and 9). The methodology described here routinely achieves blanks with ^{10}Be/^{9}Be ratios in the mid 10^{-16} level, allowing samples with ratios in the low 10^{-15} level to be measured. Decreasing the detection limits of ^{10}Be analysis by AMS opens new frontiers for the types of samples that can be studied. In particular, having lower detection limits enables the analysis of samples with little ^{10}Be, including those that are very young (Licciardi et al., 2009), those that have been subjected to rapid erosion (Portenga et al., 2015), or those that have been buried for long durations (Erlanger et al., 2012; Gibbon et al., 2014).

7. Conclusions

Analysis of quality control data associated with ~800 ^{10}Be samples prepared at the University of Vermont and measured at Lawrence Livermore National Laboratory shows that methodological optimization can yield samples that perform consistently and similarly to standards during AMS analysis. While data accuracy and precision are, to some extent, controlled by design, performance, and operation of the AMS, both are also influenced by the chemistry and sample preparation performed by cosmogenic extraction laboratories. We demonstrate that methodological optimization aimed at maximizing Be yield, while minimizing contaminants and background levels of ^{10}Be and ^{10}B, can increase data accuracy and precision and lower detection limits (although replicate analyses of internal geologic standards will further assess accuracy and precision of the chemical methods we employ here; Jull et al., 2015; Rood et al., 2014). Methodological optimization also helps to identify and address problematic samples, such as those containing native Be or high concentrations of accessory cations, and improves time efficiency of laboratory methods and AMS analysis. Such enhancements in data quality and efficiency can open new frontiers for the scientific questions that can be addressed with *in situ* produced ^{10}Be.

Acknowledgments

Method development and sample analyses described here were supported by the National Science Foundation (especially ARC-1023191 and ARC-0713956 to Bierman and EAR-0948350 to Rood) and the University of Vermont. Corbett was supported by a National Science Foundation Graduate Research Fellowship and a Doctoral

Dissertation Research Improvement Grant (BCS-1433878). We thank L. Reusser for assistance in method development, the staff of CAMS-LLNL for assistance in making ^{10}Be measurements and two anonymous reviewers for improving the manuscript.

References

Balco, G., 2011. Contributions and unrealized potential contributions of cosmogenic-nuclide exposure dating to glacier chronology, 1990–2010. Quat. Sci. Rev. 30, 3–27.

Balco, G., Briner, J., Finkel, R., Rayburn, J., Ridge, J., Schaefer, J., 2009. Regional beryllium-10 production rate calibration for late-glacial northeastern North America. Quat. Geochronol. 4, 93–107.

Balco, G., Rovey, C., 2008. An isochron method for cosmogenic-nuclide dating of buried soils and sediments. Am. J. Sci. 308, 1083–1114.

Balco, G., Stone, J., Lifton, N., Dunai, T., 2008. A complete and easily accessible means of calculating surface exposure ages or erosion rates from ^{10}Be and ^{26}Al measurements. Quat. Geochronol. 3, 174–195.

Bierman, P., Gillespie, A., Caffee, M., 1995. Cosmogenic ages for earthquake recurrence intervals and debris flow fan deposition, Owens Valley, California. Science 270, 447–450.

Bierman, P., Marsella, K., Patterson, C., Davis, P., Caffee, M., 1999. Mid-Pleistocene cosmogenic minimum-age limits for pre-Wisconsinan glacial surfaces in southwestern Minnesota and southern Baffin Island: a multiple nuclide approach. Geomorphology 27, 25–39.

Bierman, P., Nichols, K., 2004. Rock to sediment- slope to sea with ^{10}Be- rates of landscape change. Annu. Rev. Earth Planet. Sci. 32, 215–255.

Bierman, P., Steig, E., 1996. Estimating rates of denudation using cosmogenic isotope abundances in sediment. Earth Surf. Process. Landf. 21, 125–139.

Borchers, B., Marrero, S., Balco, G., Caffee, M., Goehring, B., Lifton, N., Nishiizumi, K., Phillips, F., Schaefer, J., Stone, J., 2016. Geological calibration of spallation production rates in the CRONUS-Earth project. Quat. Geochronol. 31, 188–198. http://dx.doi.org/10.1016/j.quageo.2015.01.009.

Briner, J., Young, N., Goehring, B., Schaefer, J., 2012. Constraining Holocene ^{10}Be production rates in Greenland. J. Quat. Sci. 27, 2–6.

Brown, E., Bourles, D., Raisbeck, G., Yiou, F., Burchfiel, B., Molnar, P., Qidong, D., Jun, L., 1998. Estimation of slip rates in the southern Tien Shan using cosmic ray exposure dates of abandoned alluvial fans. Geol. Soc. Am. Bull. 110, 377–386.

Brown, E., Edmond, J., Raisbeck, G., Yiou, F., Kurz, M., Brook, E., 1991. Examination of surface exposure ages of Antarctic moraines using in situ produced ^{10}Be and ^{26}Al. Geochim. Cosmochim. Acta 55, 2269–2283.

Brown, E., Stallard, R., Larsen, M., Raisbeck, G., Yiou, F., 1995. Denudation rates determined from the accumulation of in situ-produced ^{10}Be in the Luquillo Experimental Forest, Puerto Rico. Earth Planet. Sci. Lett. 129, 193–202.

Chmeleff, J., Von Blanckenburg, F., Kossert, K., Jakob, D., 2010. Determination of the ^{10}Be half-life by multicollector ICP-MS and liquid scintillation counting. Nucl. Instrum. Methods Phys. Res. B Beam Interact. Mater. At. 268, 192–199.

Clifford, D., 1999. Ion-exchange and Inorganic Adsorption, Water Quality and Treatment: a Handbook of Community Water Supplies. American Water Works Association, McGraw-Hill, New York.

Corbett, L., Bierman, P., Neumann, T., Graly, J., 2015. Inferring Glacial History and Subglacial Process Through Analysis of Cosmogenic Nuclides in Icebound Cobbles. American Geophysical Union Fall Meeting Abstract ID C11A-0745.

Ditchburn, R., Whitehead, N., 1994. The separation of ^{10}Be from silicates. In: 3rd Workshop of the South Pacific Environmental Radioactivity Association, pp. 4–7.

Erlanger, E., Granger, D., Gibbon, R., 2012. Rock uplift rates in South Africa from isochron burial dating of fluvial and marine terraces. Geology 40, 1019–1022.

Fabel, D., Harbor, J., 1999. The use of in-situ produced cosmogenic radionuclides in glaciology and glacial geomorphology. Ann. Glaciol. 28, 103–110.

Fairhall, A., 1960. The Radiochemistry of Beryllium, Nuclear Science Series. National Academy of Sciences and National Research Council, Washington, DC.

Gibbon, R., Pickering, T., Sutton, M., Heaton, J., Kuman, K., Clarke, R., Brain, C., Granger, D., 2014. Cosmogenic nuclide burial dating of hominin-bearing Pleistocene cave deposits at Swartkrans, South Africa. Quat. Geochronol. 24, 10–15.

Gosse, J., Phillips, F., 2001. Terrestrial in situ cosmogenic nuclides: theory and application. Quat. Sci. Rev. 20, 1475–1560.

Granger, D., Kirchner, J., Finkel, R., 1996. Spatially averaged long-term erosion rates measured from in situ-produced cosmogenic nuclides in alluvial sediment. J. Geol. 104, 249–257.

Granger, D., Lifton, N., Willenbring, J., 2013. A cosmic trip: 25 years of cosmogenic nuclides in geology. Geol. Soc. Am. Bull. 125, 1379–1402.

Granger, D., Muzikar, P., 2001. Dating sediment burial with in situ-produced cosmogenic nuclides: theory, techniques, and limitations. Earth Planet. Sci. Lett. 188, 269–281.

Grew, E., 2002. Beryllium in metamorphic environments (emphasis on aluminous compositions). In: Grew, E. (Ed.), Beryllium: Mineralogy, Petrology, and Geocheminstry, vol. 50. Mineralogical Society of America, Chantilly, Virginia, p. 690.

Heyman, J., Stroeven, A., Harbor, J., Caffee, M., 2011. Too young or too old: evaluating cosmogenic exposure dating based on an analysis of compiled boulder exposure ages. Earth Planet. Sci. Lett. 302, 71–80.

Hunt, A., Larsen, J., Bierman, P., Petrucci, G., 2008. Investigation of factors that affect the sensitivity of accelerator mass spectrometry for cosmogenic ^{10}Be and ^{26}Al isotope analysis. Anal. Chem. 80, 1656–1663.

Hunt, A., Petrucci, G., Bierman, P., Finkel, R., 2006. Metal matrices to optimize ion beam currents for accelerator mass spectrometry. Nucl. Instrum. Methods Phys. Res. B Beam Interact. Mater. At. 243, 216–222.

Hunt, A., Petrucci, G., Bierman, P., Finkel, R., 2007. Investigation of metal matrix systems for cosmogenic 26Al analysis by accelerator mass spectrometry. Nucl. Instrum. Methods Phys. Res. B 260, 633–636.

Jull, A.J.T., Scott, E.M., Bierman, P., 2015. The CRONUS-Earth inter-comparison for cosmogenic isotope analysis. Quat. Geochronol. 26, 3–10.

Klein, J., Middleton, R., 1984. Accelerator mass spectrometry at the University of Pennsylvania. Nucl. Instrum. Methods Phys. Res. B Beam Interact. Mater. At. 5, 129–133.

Kohl, C., Nishiizumi, K., 1992. Chemical isolation of quartz for measurement of in-situ-produced cosmogenic nuclides. Geochim. Cosmochim. Acta 56, 3583–3587.

Korschinek, G., Bergmaier, A., Faestermann, T., Gerstmann, U., Knie, K., Rugel, G., Wallner, A., Dillmann, I., Dollinger, G., Lierse von Gostomski, C., Kossert, K., Maiti, M., Poutivtsev, M., Remmert, A., 2010. A new value for the half-life of 10Be by heavy-ion elastic recoil detection and liquid scintillation counting. Nucl. Instrum. Methods Phys. Res. B Beam Interact. Mater. At. 268, 187–191.

Lal, D., 1988. In situ-produced cosmogenic isotopes in terrestrial rocks. Annu. Rev. Earth Planet. Sci. 16, 355–388.

Lanford, W., Parker, P., Bauer, K., Turekian, K., Cochran, J., Krishnaswami, S., 1980. Measurements of ^{10}Be distributions using a tandem Van De Graaff accelerator. Nucl. Instrum. Methods 168, 505–510.

Licciardi, J., Schaefer, J., Taggart, J., Lund, D., 2009. Holocene glacier fluctuations in the Peruvian Andes indicate northern climate linkages. Science 325, 1677–1679.

Matmon, A., Schwartz, D., Finkel, R., Clemmens, S., Hanks, T., 2005. Dating offset fans along the Mojave section of the San Andreas fault using cosmogenic 26Al and 10Be. Geol. Soc. Am. Bull. 117, 795–807.

Merchel, S., Arnold, M., Aumaitre, G., Benedetti, L., Bourles, D., Braucher, R., Alfimov, V., Freeman, S., Steier, P., Wallner, A., 2008. Towards more precise ^{10}Be and ^{36}Cl data from measurements at the 10^{-14} level: influence of sample preparation. Nucl. Instrum. Methods Phys. Res. B Beam Interact. Mater. At. 266, 4921–4926.

Merchel, S., Bremser, W., Akhmadaliev, S., Arnold, M., Aumaitre, G., Bourles, D., Braucher, R., Caffee, M., Christl, M., Fifield, K., Finkel, R., Freeman, S., Ruiz-Gomez, A., Kubik, P., Martschini, M., Rood, D., Tims, S., Wallner, A., Wilcken, K., Xu, S., 2012. Quality assurance in accelerator mass spectrometry: results from an international round-robin exercise for ^{10}Be. Nucl. Instrum. Methods Phys. Res. B Beam Interact. Mater. At. 289, 68–73.

Middleton, R., Klein, J., Dezfouly-Arjomandy, B., Albrecht, A., Xue, S., Herzog, G., 1994. ^{10}Be in bauxite and commercial aluminum. Nucl. Instrum. Methods Phys. Res. B Beam Interact. Mater. At. 92, 362–366.

Muzikar, P., Elmore, D., Granger, D., 2003. Accelerator mass spectrometry in geologic research. Geol. Soc. Am. Bull. 115, 643–654.

Nishiizumi, K., Imamura, M., Caffee, M., Southon, J., Finkel, R., McAninch, J., 2007. Absolute calibration of ^{10}Be AMS standards. Nucl. Instrum. Methods Phys. Res. B Beam Interact. Mater. At. 258, 403–413.

Nishiizumi, K., Kohl, C., Arnold, J., Dorn, R., Klein, I., Fink, D., Middleton, R., Lal, D., 1993. Role of in situ cosmogenic nuclides ^{10}Be and ^{26}Al in the study of diverse geomorphic processes. Earth Surf. Process. Landf. 18, 407–425.

Nishiizumi, K., Kohl, C., Arnold, J., Klein, J., Fink, D., Middleton, R., 1991. Cosmic ray produced ^{10}Be and ^{26}Al in Antarctic rocks: exposure and erosion history. Earth Planet. Sci. Lett. 104, 440–454.

Nishiizumi, K., Lal, D., Klein, J., Middleton, R., Arnold, J., 1986. Production of ^{10}Be and ^{26}Al by cosmic rays in terrestrial quartz in situ and implications for erosion rates. Nature 319, 134–136.

Nishiizumi, K., Winterer, E., Kohl, C., Klein, J., Middleton, R., Lal, D., Arnold, J., 1989. Cosmic ray production rates of ^{10}Be and ^{26}Al in quartz from glacially polished rocks. J. Geophys. Res. 94, 17907.

Ochs, M., Ivy-Ochs, S., 1997. The chemical behavior of Be, Al, Fe, Ca and Mg during AMS target preparation from terrestrial silicates modeled with chemical speciation calculations. Nucl. Instrum. Methods Phys. Res. B 123, 235–240.

Phillips, F., Zreda, M., Smith, S., Elmore, D., Kubik, P., Sharma, P., 1990. Cosmogenic chlorine-36 chronology for glacial deposits at Bloody Canyon, eastern Sierra Nevada. Science 248, 1529–1532.

Portenga, E., Bierman, P., 2011. Understanding Earth's eroding surface with ^{10}Be. GSA Today 21, 4–10.

Portenga, E., Bierman, P., Duncan, C., Corbett, L., Kehrwald, N., Rood, D., 2015. Erosion rates of the Bhutanese Himalaya determined using in situ-produced 10Be. Geomorphology 233, 112–126.

Putnam, A., Schaefer, J., Barrell, D., Vandergoes, M., Denton, G., Kaplan, M., Finkel, R., Schwartz, R., Goehring, B., Kelley, S., 2010. In situ cosmogenic 10Be production-rate calibration from the Southern Alps, New Zealand. Quat. Geochronol. 5, 392–409.

Raisbeck, G., Yiou, F., Bourles, D., Ledtringuez, J., Deboffle, D., 1987. Measurements of ^{10}Be and ^{26}Al with a tandetron AMS facility. Nucl. Instrum. Methods Phys. Res. B Beam Interact. Mater. At. 29, 22–26.

Raisbeck, G., Yiou, F., Fruneau, M., Loiseaux, J., 1978. Beryllium-10 mass spectrometry with a cyclotron. Science 202, 215–217.

Rood, D., Brown, T., Finkel, R., Guilderson, T., 2013. Poisson and non-Poisson uncertainty estimations of ^{10}Be/^{9}Be measurements at LLNL-CAMS. Nucl. Instrum. Methods Phys. Res. B 294, 426–429.

Rood, D., Hall, S., Guilderson, T., Finkel, R., Brown, T., 2010. Challenges and opportunities in high-precision Be-10 measurements at CAMS. Nucl. Instrum. Methods Phys. Res. B Beam Interact. Mater. At. 268, 730–732.

Rood, D., Xu, S., Shank, R., Dougans, A., Gallacher, P., Keefe, K., Miguens-Rodriguez, M., Bierman, P., Carlson, A., Freeman, S., 2014. Towards high precision and low ratio Be-10 measurements with the SUERC 5MV tandem: bigger isn't always better. In: The Thirteenth International Conference on Accelerator Mass Spectrometry Programme and Abstracts, 53.

Shanks, R., Freeman, S., 2015. Sputter-pits casting to measure AMS sample consumption. Nucl. Instrum. Methods Phys. Res. B Beam Interact. Mater. At. 361, 168–172.

Southon, J., Vogel, J., Nowikow, I., Nelson, D., Korteling, R., Ku, T., Kusakabe, M., Huh, C., 1983. The measurement of ^{10}Be concentrations with a tandem accelerator. Nucl. Instrum. Methods Phys. Res. 205, 251–257.

Stone, J., 1998. A rapid fusion method for separation of beryllium-10 from soils and silicates. Geochim. Cosmochim. Acta 62, 555–561.

Suter, M., 1990. Accelerator mass spectrometry: state of the art in 1990. Nucl. Instrum. Methods Phys. Res. B Beam Interact. Mater. At. 52, 211–223.

Tera, F., Brown, L., Morris, J., Sacks, S., 1986. Sediment incorporation in island-arc magmas: inferences from ^{10}Be. Geochim. Cosmochim. Acta 50, 535–550.

Thomas, J., Manglni, A., Parker, P., 1981. Improvements in an accelerator based mass spectrometer for measuring 10Be. IEEE Trans. Nucl. Sci. 28, 1478–1480.

Tuniz, C., Bird, J., Fink, D., Herzog, G., 1998. Accelerator Mass Spectrometry: Ultrasensitive Analysis for Global Science. CRC Press, Boston.

Turekian, K., Cochran, J., Krishnaswami, S., Lanford, W., Parker, P., Bauer, K., 1979. The measurement of 10Be in manganese nodules using a tandem Van De Graaff accelerator. Geophys. Res. Lett. 6, 417–420.

von Blanckenburg, F., 2005. The control mechanisms of erosion and weathering at basin scale from cosmogenic nuclides in river sediment. Earth Planet. Sci. Lett. 237, 462–479.

von Blanckenburg, F., Willenbring, J., 2014. Cosmogenic nuclides: dates and rates of earth-surface change. Elements 10, 341–346.